

# Computer Physics

## Report No. 8

Dominik Papaj

December 26, 2025

## 1 Introduction

Molecular dynamics (MD) is a numerical method for simulating the motion of interacting particles by solving Newton's equations of motion. In this work, a two-dimensional system of argon atoms confined in a square box is considered in order to reproduce basic physical properties of atomic gases and solids.

Interatomic interactions are described by the Lennard–Jones (LJ) potential, which accounts for short-range repulsion and long-range attraction between neutral atoms:

$$U_{\text{LJ}}(r) = 4\epsilon \left[ \left(\frac{\sigma}{r}\right)^{12} - \left(\frac{\sigma}{r}\right)^6 \right]. \quad (1)$$

The force acting on each particle is obtained from the gradient of the potential,

$$\vec{F}_i = -\nabla_{\vec{r}_i} U. \quad (2)$$

The temporal evolution of the system is determined by integrating the equations of motion,

$$m \frac{d^2 \vec{r}_i}{dt^2} = \vec{F}_i, \quad (3)$$

using the velocity–Verlet integration scheme. Periodic boundary conditions are employed to reduce finite-size effects and to approximate an infinite system.

The study is organized into several stages. First, the correctness of the initial conditions and energy conservation is examined. Subsequently, a Nose–Hoover thermostat is applied to control the temperature and analyze thermalization. The resulting velocity distribution is compared with the analytical Maxwell–Boltzmann distribution. Finally, a cooling procedure is implemented to investigate crystallization and structural ordering in the system.

All simulations are performed using reduced Lennard–Jones units, which simplify the equations of motion and improve numerical stability.

## 2 Numerical Method

### 2.1 Reduced Units (Sec. 1.1)

The simulations are carried out using reduced Lennard–Jones units appropriate for argon. The reference mass, energy, and length are chosen as

$$m = 1, \quad \epsilon = 1, \quad \sigma = 1, \quad (4)$$

and the Boltzmann constant is set to

$$k_B = 1. \quad (5)$$

Temperature is rescaled using

$$T = \frac{T[\text{K}]}{T_{\text{ref}}}, \quad T_{\text{ref}} = 119 \text{ K}. \quad (6)$$

With this choice, all physical quantities become dimensionless and are expressed in effective units.

## 2.2 Initial Positions and Velocities (Sec. 1.2)

Initial particle positions are placed on a regular square lattice inside a box of width  $L$ . This avoids placing particles too close to each other, which would result in very large forces and numerical instability.

Initial velocities are assigned using the Maxwell–Boltzmann distribution. Each velocity component is drawn from a normal distribution with zero mean and variance

$$\sigma_v^2 = \frac{k_B T}{m}. \quad (7)$$

To remove artificial drift of the system, the center-of-mass velocity

$$\vec{v}_{\text{cm}} = \frac{1}{N} \sum_{i=1}^N \vec{v}_i \quad (8)$$

is computed and subtracted from all particle velocities.

## 2.3 Lennard–Jones Forces and Potential Energy (Sec. 1.3)

Particles interact through a shifted Lennard–Jones potential with cutoff radius  $r_{\text{cut}}$ . The shifted form ensures that both the potential and force smoothly go to zero at the cutoff. Interactions are calculated only for particle pairs with

$$r_{ij} < r_{\text{cut}}. \quad (9)$$

Periodic boundary conditions are implemented using the minimum image convention. The force on each particle is obtained by summing all pairwise forces, while Newton’s third law is used to reduce computational cost.

The total potential energy of the system is

$$E_{\text{pot}} = \sum_{i < j} U_{\text{LJ}}^{\text{shift}}(r_{ij}). \quad (10)$$

## 2.4 Kinetic Energy and Temperature (Sec. 1.4)

The kinetic energy is calculated as

$$E_{\text{kin}} = \sum_{i=1}^N \frac{1}{2} m(v_{x,i}^2 + v_{y,i}^2). \quad (11)$$

Using the equipartition theorem, the instantaneous temperature is given by

$$T = \frac{E_{\text{kin}}}{N k_B}. \quad (12)$$

## 2.5 Time Integration and Thermostat (Sec. 1.5)

The equations of motion are integrated using the velocity–Verlet algorithm, which updates velocities in two half steps around a full position update. This method is time–reversible and conserves energy well for small time steps.

Temperature control is achieved using a Nose–Hoover thermostat. The coupling strength to the heat bath is controlled by the parameter  $Q$ . Large values of  $Q$  correspond to nearly microcanonical dynamics, while smaller values enforce stronger temperature control.

## 2.6 Velocity Distribution (Sec. 1.6)

The velocity magnitude distribution is obtained by collecting particle velocities during the simulation and constructing a histogram. For a two-dimensional ideal gas, the analytical Maxwellian distribution is

$$f(v) = \frac{m}{k_B T} v \exp\left(-\frac{mv^2}{2k_B T}\right). \quad (13)$$

The numerical histogram is normalized and compared directly with this analytical expression to verify the correctness of the simulation.

## 3 Results

Table 1: Main simulation parameters (reduced LJ units).

Box width	$L = 25$
Number of atoms	$N = 201$
Time step	$\Delta t = 0.002$
Cutoff radius	$r_{\text{cut}} = 2.7$
Reference temperature	$T_{\text{ref}} = 119$ K
Mass, energy, length	$m = \varepsilon = \sigma = 1$ (reduced units)

## Task 1 — Initial conditions

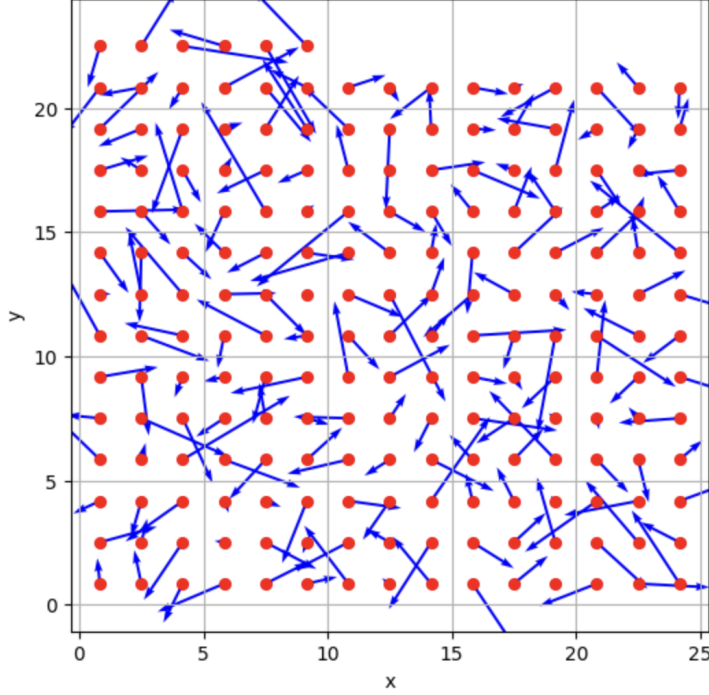


Figure 1: Initial particle positions (red dots) placed on a regular square lattice. Blue arrows show the velocity vectors sampled from the Maxwell–Boltzmann distribution and corrected by removing the centre–of–mass drift.

The initial configuration (Fig. 1) shows particles placed on a square lattice with uniform spacing; no overlaps are present, so initial potential energies are moderate and the time step is safe. The velocity field was drawn from a Gaussian with  $\sigma_v = \sqrt{k_B T/m}$  and the centre–of–mass velocity was subtracted, as required.

## Task 2 — Energy conservation and single particle trajectory

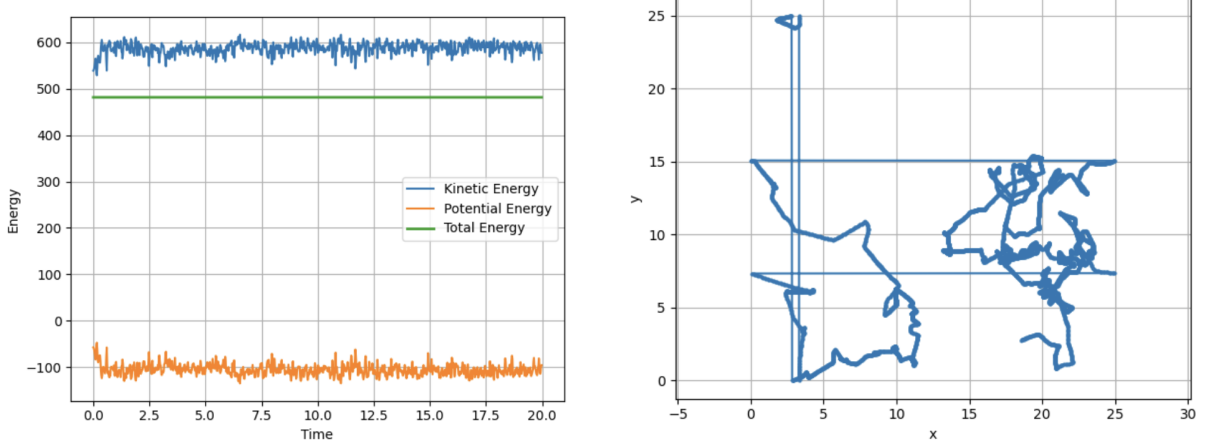


Figure 2: Left: kinetic, potential and total energy vs. time for the microcanonical run ( $Q \rightarrow \infty$ ). Right: trajectory of a single particle (index  $N/2$ ).

Energy is conserved to numerical precision: the total energy remains essentially constant while kinetic and potential energies exchange (left panel). The single-particle trajectory (right panel) is chaotic/diffusive — collisions with neighbors change direction frequently and the particle crosses the periodic box many times, consistent with low-density gas-like dynamics.

### Task 3 — Thermalization with Nose–Hoover

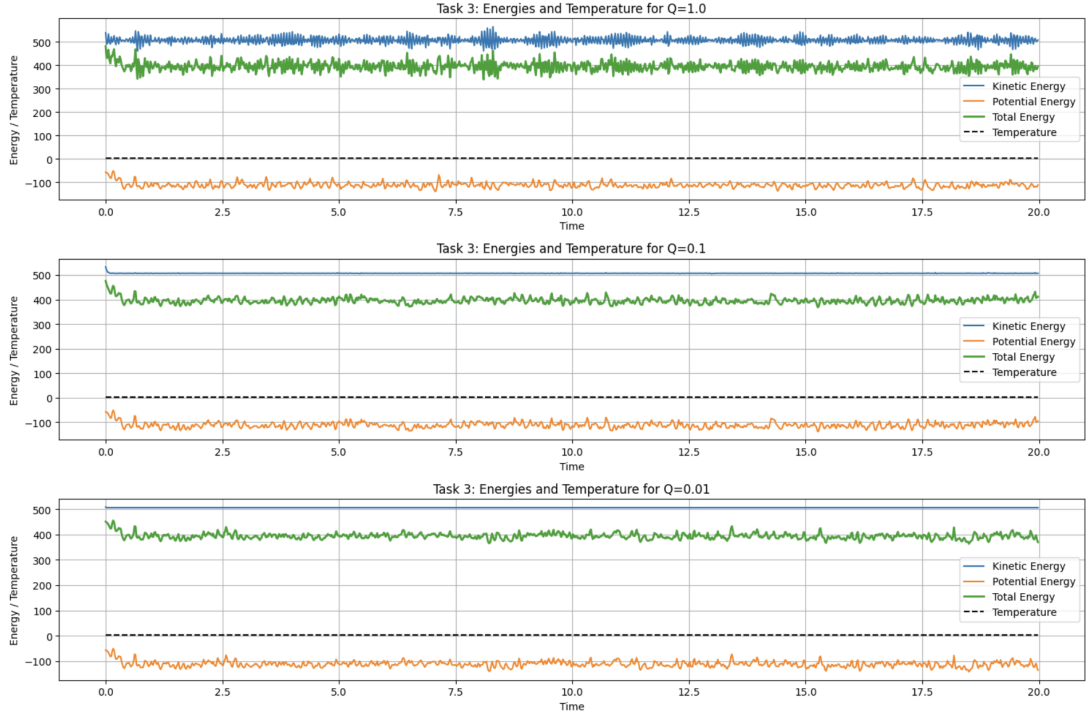


Figure 3: Energies and instantaneous temperature for three thermostat couplings  $Q$  (up to down:  $Q = 1$ ,  $Q = 0.1$ ,  $Q = 0.01$ ).

Stronger coupling (smaller  $Q$ ) leads to faster and tighter temperature control: for  $Q = 0.01$  the instantaneous temperature and kinetic energy fluctuations are strongly suppressed compared to  $Q = 1$  (Fig. 3). For large  $Q$  the dynamics is essentially microcanonical and the temperature fluctuates more.

### Task 4 — Velocity histograms vs. Maxwellian

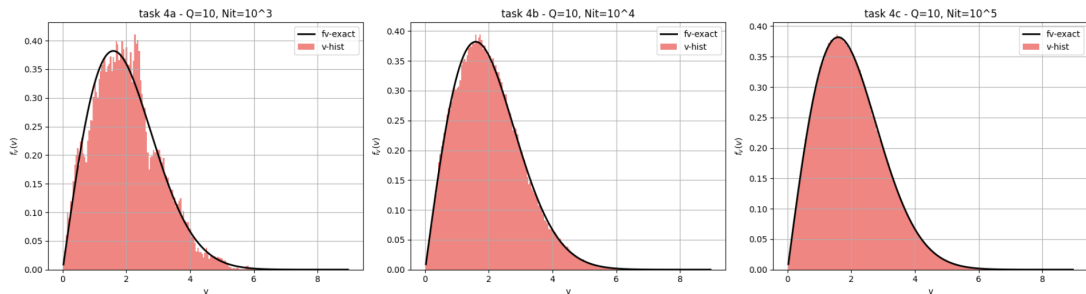


Figure 4: Velocity histograms for  $Q = 10$  and increasing sampling length (left to right:  $N_{it} = 10^3, 10^4, 10^5$ ). Red bars: numerical histogram; black curve: analytical Maxwellian  $f(v) = \frac{m}{k_B T} v \exp(-mv^2/2k_B T)$ .

The numerical histograms converge to the analytical Maxwellian as the sampling increases (Fig. 4). Small deviations remain due to finite statistics and due to interparticle interactions (the system is not an ideal non-interacting gas), but the agreement is good already for  $N_{\text{it}} = 10^4$ .

### Task 5 — Cooling and crystallization

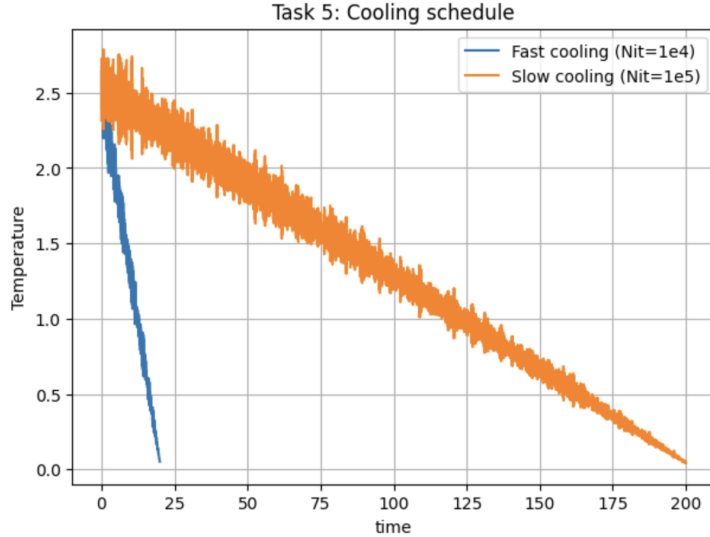


Figure 5: Instantaneous temperature vs. time for fast ( $N_{\text{it}} = 10^4$ ) and slow ( $N_{\text{it}} = 10^5$ ) cooling schedules.

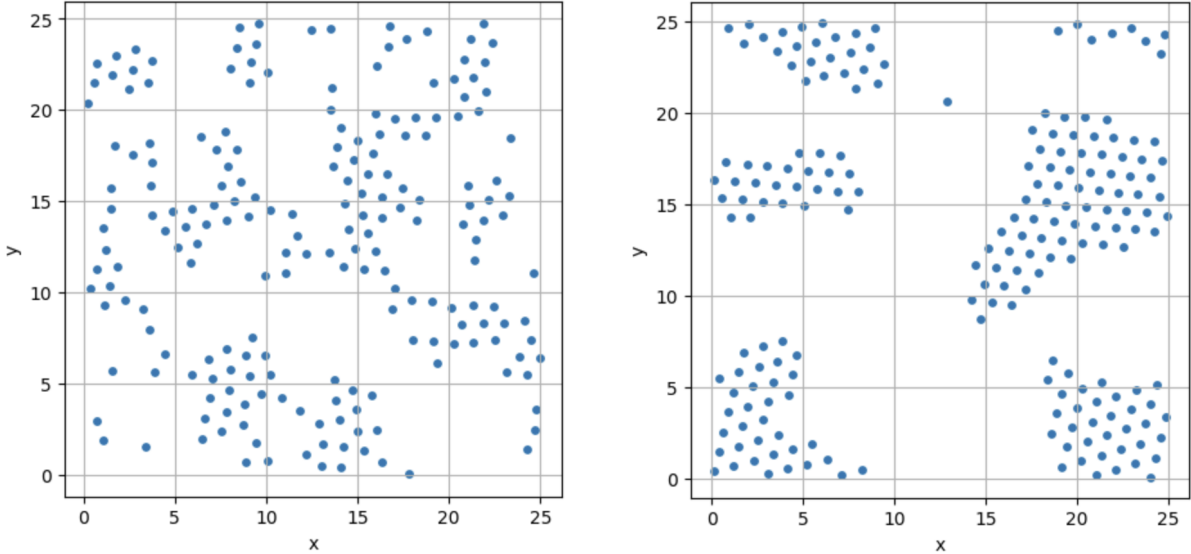


Figure 6: Final atomic positions after (left) fast cooling and (right) slow cooling. Slow cooling allows rearrangement into more ordered (lower energy) structures.

Under a fast cooling schedule the system is typically trapped in a high-energy disordered state (left), while slow cooling gives atoms time to minimize potential energy and form more ordered crystalline domains (right). This demonstrates the competition between kinetics (cooling rate) and thermodynamic ordering.

## 4 Conclusions

A two-dimensional molecular dynamics simulation of argon atoms interacting via the Lennard–Jones potential was successfully implemented. The velocity–Verlet algorithm together with periodic boundary conditions provided stable dynamics, and in the microcanonical limit the total energy was conserved to numerical precision. Kinetic and potential energies exchanged as expected, confirming the correctness of the force calculations and time integration.

Velocity distributions obtained from the simulations converge toward the analytical Maxwellian form with increasing sampling length. The Nose–Hoover thermostat correctly controls the system temperature: large coupling parameters lead to near-microcanonical behaviour, while strong coupling suppresses temperature fluctuations. Cooling simulations demonstrate that slow cooling allows the system to reach more ordered, lower-energy configurations, whereas fast cooling traps the system in disordered states.

Overall, the results are consistent with theoretical expectations and illustrate how molecular dynamics simulations connect microscopic particle motion with macroscopic thermodynamic behaviour.